Hsc70 Contacts Helix III of the J Domain from Polyomavirus T Antigens: Addressing a Dilemma in the Chaperone Hypothesis of How They Release E2F from pRb†

Ravindranath Garimella,‡ Xin Liu,‡ Wei Qiao,‡ Xiangyang Liang,‡ Erik R. P. Zuiderweg,§ Michael I. Riley,|| and Steven R. Van Doren*,‡

Department of Biochemistry, 117 Schweitzer Hall, and Department of Veterinary Pathobiology, E158 Veterinary Medicine, University of Missouri, Columbia, Missouri 65211, and Biophysics Research Division and Departments of Chemistry and Biological Chemistry, 930 North University Avenue, The University of Michigan, Ann Arbor, Michigan 48109-1055

Received March 1, 2006; Revised Manuscript Received April 14, 2006

ABSTRACT: Hsc70's expected binding site on helix II of the J domain of T antigens appears to be blocked in its structure bound to tumor suppressor pRb. We used NMR to map where mammalian Hsc70 binds the J domain of murine polyomavirus T antigens (PyJ). The ATPase domain of Hsc70 unexpectedly has its biggest effects on the NMR peak positions of the C-terminal end of helix III of PyJ. The Hsc70 ATPase domain protects the C-terminal end of helix III of PyJ from an uncharged paramagnetic probe of chelated Gd(III), clearly suggesting the interface. Effects on the conserved HPD loop and helix II of PyJ are smaller. The NMR results are supported by a novel assay of Hsc70's ATP hydrolysis showing that mutations of surface residues in PyJ helix III impair PyJ-dependent stimulation of Hsc70 activity. Evolutionary trace analysis of J domains suggests that helix III usually may join helix II in contributing specificities for cognate hsp70s. Our novel evidence implicating helix III differs from evidence that *Escherichia coli* DnaK primarily affects helix II and the HPD loop of DnaJ. We find the pRb-binding fragment of E2F1 to be intrinsically unfolded and a good substrate for Hsc70 in vitro. This suggests that E2F1 could be a substrate for Hsc70 recruited by T antigen to an Rb family member. Importantly, our results strengthen the chaperone hypothesis for E2F release from an Rb family member by Hsc70 recruited by large T antigen. That is, it now appears that Hsc70 can freely access helix III and the HPD motif of large T antigen bound to an Rb family member.

The pRb[1] family of tumor suppressors (pocket proteins pRb, p107, and p130) sequester E2F family transactivators of the genes for initiating and sustaining DNA replication (*1*, *2*). E2Fs 1−3 together are required for cell proliferation (*3*). Transactivation of E2F-regulated promoters by freed activator E2Fs such as E2F1 likely follows release of E2F-containing repressor complexes from the promoters (*4*). Release of E2Fs from pRb and other pocket proteins may be essential for the rapid growth of tumor cells (*1*). How papovaviruses, i.e., DNA tumor viruses such as papillomaviruses and polyomaviruses, override pRb family sequestration of E2Fs to promote advancement of the host cell cycle into S-phase is incompletely resolved. The polyomavirus SV40 is associated with higher risk of primary cancers of brain and bone, malignant mesothelioma, and non-Hodgkin's lymphoma (*5*). Brodsky and Pipas postulated that polyomaviruses use the J domain of their T antigens to recruit Hsc70 to the multiprotein complex target (*6*). Energy for the action upon the targeted complex was suggested to come from Hsc70's hydrolysis of ATP. This general chaperone hypothesis has been applied specifically to a T antigen-dependent freeing of E2Fs from pRb family members (*7*, *8*). The J domain of large T antigen, Hsc70, and its hydrolysis of ATP were indeed found necessary for the release of E2Fs from pRb family members and ensuing E2F-dependent transcriptional activation (*9*, *10*).

Understanding of T antigens' dependence upon their J domain for Hsc70 recruitment (*7*, *11*) relies upon structural and functional analogy with *E. coli* DnaJ. Evidence to date has suggested the center of helix II of DnaJ and the conserved HPD motif to be the main interface with the DnaK example of hsp70s (*12*, *13*). However, helix II of the J domain of SV40's large T antigen is largely buried in the crystallographic structure of the N-terminal fragment (NT) of large T antigen bound to the pRb pocket domain (*8*); this steric

† This work was supported by American Cancer Society Grant RSG-98-253-4-MBC to S.R.V.D. E.R.P.Z. acknowledges DHHS Grant R01GM63027 for support. The 600 MHz NMR spectrometer and cryogenic probe used were purchased with funding from NSF Grant DBI-0070359, DHHS Grant R01GM5728, and the University of Missouri.

* Address correspondence to this author. E-mail: vandorens@missouri.edu. Tel: (573) 882-5113. Fax: (573) 884-4812.

‡ Department of Biochemistry, University of Missouri.

§ Biophysics Research Division and Departments of Chemistry and Biological Chemistry, The University of Michigan.

|| Department of Veterinary Pathobiology, University of Missouri.

[1] Abbreviations: DTPA-BMA, diethylenetriaminepentaacetic acid bismethylamide; ET, evolutionary trace analysis; Hsc70, heat shock cognate of 70 kDa; MRI, magnetic resonance imaging; NMR, nuclear magnetic resonance spectroscopy; NT, N-terminal fragment of large T antigen; pRb, retinoblastoma tumor suppressor protein; PyJ, N-terminal J domain shared among the T antigens of murine polyomavirus; SV40, simian virus 40; TROSY, transverse relaxation-optimized spectroscopy.

10.1021/bi060411d CCC: $33.50
Published on Web 05/17/2006

hindrance was noted (*14*). Steric hindrance to helix II of the J domain would therefore *appear* to interfere in Hsc70 docking with large T antigen that is bound to pRb. Here we show by NMR spectroscopy that there need *not* be direct competition between Hsc70 and pRb. Hence the ternary and quaternary complexes of the chaperone hypothesis (*6*−*8*) are possible.

DnaJ-like proteins are categorized in three types according to domain structure. Type I J domains share all four domains of *Escherichia coli* DnaJ (*15*). Type II, e.g., Hsp40 (HDJ-1), have the J domain and Gly-Phe-rich linker. Type III, such as found in T antigens, contain only the J domain among other domains (*15*). The HPD motif is conserved among almost all J domains (*13*) and is required for stimulation of hsp70s (*11*, *16*, *17*).

Considerable disparities exist in other features of J domains reported to be important to interaction with hsp70s. The positively charged helix II of *E. coli* DnaJ was found to be a principal site of interaction with DnaK (*12*). The key positive charge on helix II was proposed to be Lys35 in the numbering of polyomavirus T antigens (PyJ), corresponding to Lys26 in DnaJ numbering (*18*). The importance of Lys26 of *E. coli* DnaJ and neighboring residues Tyr25 and Phe47 of helix III was demonstrated (*19*). Some helix III residues of DnaJ were affected in NMR titrations with the ATPase domain of DnaK (*12*, *20*). In the J domain of SV40 T antigens, mutations of residues 51, 53, 55, 56, and 59 suggest that helix III participates in Hsc70 interaction (*21*). In the J domain of polyomavirus large T antigen, conservative substitutions of Gln32, Ala33, Tyr34 (helix II), His49, Met52, or Asn56 (helix III) impair both pRb/E2F-dependent transactivation and cyclin A promoter transactivation (*22*). The QKRAA motif of bacterial J domains, spanning the III/IV loop and helix IV, was also implicated in interactions with DnaK and a mammalian hsp70 (*23*−*27*). Roughly corresponding to this region is the C-terminal end of helix III of J domains of viral T antigens (*18*). In summary, the HPD motif, helix II, and possibly helix III have been deemed primary sites of interaction with the ATPase domain of hsp70s, while helix IV and even helix I have been hypothesized to interact with the peptide binding domain of hsp70s (*28*).

NMR is capable of mapping interfaces of protein−protein interactions (*29*−*31*). There has been a need for NMR study of transient interactions of mammalian hsp70s with J domains, including from a viral T antigen. A favorite method of mapping interfaces is to monitor shifts of amide NMR peak positions. However, the method also responds to binding-linked adjustments in conformation (*32*, *33*). Peaks with greater than average broadening upon formation of a complex suggest residues in an interface (*34*). We developed a method that more accurately identifies the interface in a protein−protein complex (*32*, *35*). The method monitors the protection of the interface from the NMR line broadening effects of a paramagnetic probe (*32*). The agent is an uncharged chelate of Gd(III) that has the virtues of strongly broadening NMR peaks, being inert and affecting the entire accessible surface (*32*, *36*). The approach is illustrated schematically in Figure S1 of Supporting Information. This approach proved accurate in mapping interfaces in protein−protein complexes with dissociation constants of 3 nM (*35*) and ~10 μM (*37*).

Evolutionary trace analysis (ET) is a bioinformatics approach to predicting biomolecular interfaces. ET has consistently predicted well the functional surfaces of protein families with a large multiple sequence alignment (*38*−*42*). This approach identifies sequence positions conserved *within* each protein subfamily but which *can vary between subfamilies.* These positions characteristic of protein subfamilies were named "trace" or "class-specific" residues, are expected to confer specificity to that subfamily, and cluster with conserved residues at recognition sites (*38*).

Here we present the first NMR mapping of the surface of a J domain recognizing a *mammalian* hsp70, i.e., the ATPase domain of Hsc70. We used the N-terminal J domain shared among the T antigens of murine polyomavirus that we refer to as PyJ (*18*). It is homologous to the J domain of T antigens from the SV40 pathogen of primates including humans. Application of NMR approaches listed above and mutagenesis suggests that, contrary to expectation, the Hsc70 ATPase domain may contact the C-terminal end of helix III of PyJ more extensively and intimately than it contacts helix II. Our application of ET suggests that a similar set of residues found on helices II, III, and IV tunes the specificity of J domains in general. [J domains are known to select among hsp70s (*43*, *44*).] On one hand, the importance of helix III is surprising. On the other hand, our results strongly support and clarify the chaperone model of T antigen- and Hsc70-dependent release of E2F1 from pRb in the following respects. The importance of helix III of PyJ in Hsc70 recognition largely resolves the apparent problem of steric hindrance to Hsc70 reaching helix II of the J domain of T antigen bound to pRb. T antigen is hypothesized to position Hsc70 for direct action upon an E2F bound to a pocket protein such as pRb. Consistent with this hypothesis, the pRb-binding region of E2F1 (aa 243−437) is demonstrated to be an excellent substrate for Hsc70 in vitro, possibly because of an inherently unfolded region.

EXPERIMENTAL PROCEDURES

Protein Expression, Purification, and Preparation for NMR. PyJ was expressed in BL21(DE3) from a synthetic gene encoding residues 1−79 shared by murine polyomavirus T antigens, plus a six-histidine tag at the C-terminus. The predicted MW is 9985 Da (*18*). PyJ was labeled with ^{15}N using M9 medium containing [^{15}N]NH_4Cl (Isotec, Miamisburg, OH), supplemented with 20% (v/v) ^{15}N-enriched Celtone N (Spectra Stable Isotopes). Samples also enriched with ^{13}C used an equivalent medium with uniformly ^{13}C-enriched glucose (Isotec) and Celtone CN. PyJ was purified as described (*18*) but with insertion of a Q-Sepharose Fast-Flow column (GE Healthcare) between NTA (Qiagen) and Superdex 75 (GE Healthcare) chromatography steps. The Q-Sepharose column, equilibrated with 25 mM Tris-HCl (pH 7.2) and 25 mM NaCl, decreased gradual trace proteolysis by capturing traces of *E. coli* proteases while the PyJ flowed through the column without capture. The typical yield of PyJ was about 12 mg/mL per liter of culture.

The ATPase domain (aa 1−386) of bovine Hsc70 was expressed from the vector generously given by Prof. D. B. McKay. It is virtually identical in sequence with murine or human Hsc70. It has a predicted MW of 42457 Da. The ATPase domain was prepared by a modification of the

McKay laboratory's protocol (*45*, *46*). The chromatography steps employed DEAE (Bio-Rad), ATP agarose (Sigma), and hydroxyapatite (Bio-Rad) supports. The typical yield was about 40 mg/L of culture.

For NMR, both ^{15}N PyJ and Hsc70 ATPase domain were prepared in 20 mM Tris-HCl (pH 7.2 at 25 °C), 25 mM KCl, 5 mM $MgCl_2$, and 5 mM ADP. To decrease trace proteolysis of PyJ in the presence of the recombinant Hsc70 ATPase domain, a cocktail of the protease inhibitors pepstatin, leupeptin, AEBSF, TPCK, and E-64 was added to both proteins. EDTA was avoided because of the need for Mg^{2+} counterion for the nucleotide in the ATPase domain. PyJ was concentrated to about 0.6 mM and Hsc70 to about 1.8 mM. D_2O was added to 7% (v/v). Shigemi tubes were used for all experiments. Titrations were performed at 30 °C.

NMR Peak Assignments. HNCA, HN(CO)CA, HNCACB, CBCA(CO)NH, and ^{15}N NOESY-HSQC spectra were used to update peak assignments for the pH 7.2 conditions used to study interactions with the unlabeled Hsc70 ATPase domain. Spectra were collected on a 600 MHz Varian Inova spectrometer equipped with a cryogenic probe. NMRPipe was used for data processing (*47*). SPARKY was used for spectral analysis (*48*).

We used three types of NMR assays of the surface of ^{15}N-labeled PyJ affected by the unlabeled ATPase domain (aa 1−386) of bovine Hsc70 in the presence of ADP: (i) chemical shift perturbation, (ii) line broadening suggested by greater drop in peak height at potential contact sites (*34*), and (iii) protection from paramagnetic line broadening by chelated Gd(III) (*32*, *35*). ^{15}N TROSY (*49*) was the preferred means of detecting the amide peaks of ^{15}N PyJ, free and bound to the ATPase domain. The ^{15}N line sharpening of TROSY decreased overlap in PyJ spectra.

Chemical Shift Perturbation of PyJ by Hsc70. Titrations of PyJ with the Hsc70 ATPase domain (aa 1−386) exhibited slow exchange behavior at pH 7.2. Consequently, ^{15}N NOESY-HSQC was helpful in confirming peak assignments in the Hsc70-saturated state of PyJ. However, the assignments of a few peaks could not be confirmed in the bound state due to line broadening discussed below or due to high mobility of the C-terminal linker. Hsc70 ATPase domain-induced changes in amide peak position of ^{15}N PyJ are reported as a combination of the changes in ^{1}H and ^{15}N dimensions. The radial shift, $\Delta\omega_{NH}$ (in ppm), is calculated to scale the ^{15}N chemical shift changes $\Delta\omega_N$ down to the approximate scale of the ^{1}H chemical shift changes $\Delta\omega_H$:

$$\Delta\omega_{NH} = [(\Delta\omega_H)^2 + (\Delta\omega_N/6)^2]^{1/2} \quad (1)$$

PyJ Line Width Increases by Hsc70. These were assessed qualitatively as the ratio of peak height in the bound or Hsc70-saturated state to the peak height of PyJ in its free state at pH 7.2.

Hsc70 Protection of the PyJ Surface from the Paramagnetic Probe. We developed a very accurate means of mapping of protein−protein interfaces using exclusion of an inert paramagnetic NMR line broadening agent, chelated Gd(III) (*32*, *35*). This method nonselectively probes the entire solvent-accessible protein surface. The Gd(III) chelate chosen was Gd(DTPA-BMA) (*36*), used widely in magnetic resonance imaging of patients under the trade name of Omniscan (GE Healthcare, Princeton, NJ). Its electron spin $S = {}^7/_2$ is very effective in ^{1}H relaxation, a property long exploited for contrast in MRI and more recently for probing protein surfaces (*32*). The uncharged, inert character and other favorable properties of Gd(DTPA-BMA) were described (*36*). Stock solutions of Omniscan were 0.5 M and adjusted to pH 7.2 before usage. The line broadening effects of 1, 2, 3, 4, and 5 mM Gd(DTPA-BMA) on PyJ samples were measured. The peak heights were normalized by the heights in a reference spectrum without addition, for comparing each state. The normalization enables comparison of the surface accessibility of the ^{15}N-labeled protein by taking the differences between free and bound states of the protein. The slower tumbling of a complex results in greater line broadening by a paramagnetic agent (*32*). The greater overall line broadening resulting from the slower tumbling of the complex of PyJ with the Hsc70 nucleotide-binding domain has been empirically corrected for by choosing slightly lower [Gd(DTPA-BMA)] (*32*). Gd(DTPA-BMA) (3 mM) appears to broaden the lines of PyJ in the complex to a similar degree as 4 mM Gd(DTPA-BMA) for free PyJ. TROSY was used for detection as it resolves more amide peaks for quantitative comparison.

Stability of the Complex. After addition of saturating quantities of the ATPase fragment of Hsc70, samples remained stable from overnight to a few weeks. The high sensitivity of a cryogenic probe ensured that the spectra were collected prior to appreciable change. The lifetimes of the complex were limited by gradual trace proteolysis we consider to originate from our Hsc70 ATPase preparations. This occurred despite the high chromatographic purity of the proteins, the high stability of the Hsc70 ATPase domain, and use of a potent cocktail of five protease inhibitors. The data of Figures 1−3 were collected using samples of the PyJ complex with the Hsc70 ATPase domain that remained stable for about 3 weeks. The four or five small peptide degradation peaks present were easily distinguished from intact free and Hsc70-bound PyJ peaks by these criteria: The traces of four or five peptide peaks had random coil peak positions and sharp lines, failed to grow or diminish in proportion to [Hsc70] the way intact PyJ peaks did, were far from free-state PyJ peaks, and lacked the sequential NOEs of intact PyJ.

Colorimetric ATPase Assay and Protein Components. The chaperone reactions were incubated at 40 °C in a buffer of 10 mM Tris-HCl (pH 7.6), 150 mM NaCl, 4.5 mM $MgCl_2$, 1.5 mM $CaCl_2$, 1 mM dithiothreitol, and 0.1 mM phenylmethanesulfonyl fluoride. Time points were withdrawn at 0, 15, 30, 45, 60, 75, 90, 105, and 120 min. P_i formation from the ATP hydrolysis was detected colorimetrically at 660 nm at room temperature by a slight modification of the method of refs *50* and *51*. The detection solution was composed of 0.045% malachite green hydrochloride, 4.2% ammonium molybdate in 4 M HCl, 34% sodium citrate dihydrate, with 0.1% Triton X-100 substituting as nonionic detergent. All reagents were from Sigma.

PyJ was prepared as described above. Human E2F1 (aa 243−437) was expressed as a GST fusion from pGEX-6p-1-E2F1 (*52*) and purified using glutathione resin (Sigma). GST was removed using the PreScission 3C protease (GE Healthcare) and glutathione resin. Human Hsc70 and human Hsp40 (HDJ-1) were purchased from Stressgen.

Mutagenesis. Site-directed mutations were introduced to PyJ using the QuikChange mutagenesis kit (Stratagene) as described by the manufacturer. Sequencing confirmed the mutations and absence of stray mutations elsewhere.

Evolutionary Trace Analysis. Starting from 1474 sequences from the superfamily of J domains available at the time (see www.sanger.ac.uk/cgi-bin/Pfam/getacc?PF00226), we deleted sequences that were duplicated, most divergent, truncated, or lacking sequence for helix III. Alignment of the refined set of sequences, using ClustalW (www.ebi.ac.uk/clustalw), divided them into three major groups of 499, 199, and 81 sequences each. From 202 sequences of J domains from viruses, many redundant sequences were deleted, as well as 3 divergent ones. The remaining 16 distinct and representative viral J domain sequences were aligned within the second major subgroup of 199 Pfam sequences. Evolutionary trace analysis proceeded on the group of 499 sequences and group of 199 sequences, since NMR or crystal structures are available for representatives of these two groups.

Residues characteristic of subfamilies are named class-specific or trace residues (*38*, *42*). The multiple sequence alignments of the 499-member and 199-member groups were submitted separately to the evolutionary trace server at www-cryst.bioc.cam.ac.uk/~jiye/evoltrace/evoltrace.html. For each group, the phylogenetic tree was divided into 10 trace levels of sequence identity. An original rule of ET is that a class-specific position be fully conserved *within* each subfamily (*38*). Due to very low sequence homology among the superfamily of J domains, we relaxed this rule to define a class-specific position as having conservation within 85% or more of the subfamilies as proposed (*53*), a simplification of the concept of weighted ET (*54*).

RESULTS

Region of PyJ with NMR Peaks Most Shifted by the Hsc70 ATPase Domain. In the presence of 5 mM ADP at pH 7.2 at 30 °C, TROSY spectra of ^{15}N PyJ were collected with progressive additions of the Hsc70 ATPase domain to ratios of 1:0, 1:0.15, 1:0.3, 1:0.5, 1:0.7, 1:1, and 1:1.3 PyJ to Hsc70. A second set of peaks appeared for the bound state, with peak heights proportional to the Hsc70 ATPase domain added. The peaks of the free state diminished in proportion. This indicates the titrations at pH 7.2 are in slow exchange, i.e., with rate of exchange between free and bound states slower than the chemical shift differences between the peaks of the free and bound states. The chemical shift differences $\Delta\omega_{NH}$ are plotted in Figure 1a. The amide NMR peaks of PyJ residues in helix III and the C-terminal linker are those most shifted upon addition of the ATPase domain. The PyJ (T antigen) residues with peaks shifted the most, i.e., with radial shift $\Delta\omega_{NH} \geq 0.10$ ppm, are Leu51, Met52, Lys63 to Glu65, Asn72, Gly74, and Gln79 (Figure 1a). Residues with more modest Hsc70-induced $\Delta\omega_{NH}$ include Val4, Leu5, Phe27, conserved Asp44, Trp59 to Thr61, Met71, and Gly75 to Gly77. Some residues of helices I and II and the I−II loop show still more subtle shifts. Significantly, no shift was observed for the backbone NH moiety of conserved His42. With the nucleotide-binding domain bound, Leu51 and Met71 each appear to have two amide peaks, suggestive of alternate conformers. Hsc70-linked spectral effects of shifts

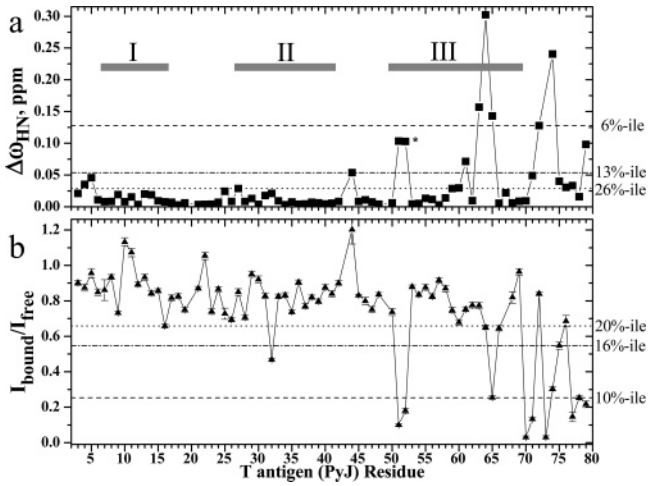

FIGURE 1: Effects of the Hsc70 ATPase domain upon the (a) NMR peak positions and (b) peak heights of PyJ backbone amide groups. In (a), the Hsc70-induced radial change in peak position between free ^{15}N PyJ and Hsc70 ATPase-saturated states of ^{15}N PyJ uses eq 1. $\Delta\omega_N$ is given for only the final addition of the Hsc70 nucleotide-binding domain, since titrations at pH 7.2 are in slow exchange. The 6 percentile most shifted amide peaks are bounded by the dashed line, the 13 percentile most shifted by the dash−dotted line, and the 26 percentile most shifted by the dotted line. The asterisk for Met52 indicates higher uncertainty from the weakness of its peak in the bound state. In (b), peak heights of free ^{15}N PyJ are divided by those of PyJ in the presence of a 1.3-fold excess of the ATPase domain of Hsc70. The 10 percentile most decreased amide peaks fall at or below the dashed line, the 16 percentile most decreased below the dash−dotted line, and the 20 percentile most decreased below the dotted line. ^{15}N TROSY spectra of PyJ were collected at pH 7.2 in the presence of 5 mM ADP at 30 °C at 600 MHz with a cryogenic probe.

or broadening affect half the residues of helix III. This suggests that helix III may be important in recognizing Hsc70, in addition to essential Asp44 of the conserved HPD motif.

The slow exchange behavior implies a relatively slow off-rate at pH 7.2. The sites of slow exchange with smaller chemical shift differences $\Delta\nu$ suggest a lower limit on the off-rate. Conservatively, $k_{off} < 2\pi\Delta\nu$, where $\Delta\nu_N \approx 18-24$ Hz in the smaller clear cases of slow exchange, namely, Val66 and Leu5. At lower pH values approaching the predicted p*I* of 6.4 of the Hsc70 ATPase domain, titrations are in fast exchange, implying a faster off-rate. The backbone amide peak of essential Asp44 shifts significantly with pH.

Since J domains promote ATP hydrolysis by hsp70 partners, J domains may prefer to bind the hsp70 when ADP is bound. We tested this expectation with the control of a titration in the presence of 5 mM ATP. The biggest shift of an amide peak of PyJ in the presence of ATP-saturated Hsc70 is from Asp44 of the conserved HPD motif. It reached a radial $\Delta\omega_{NH}$ change of 0.12 ppm at 1.3-fold excess of the ATPase domain (Figure S2 of Supporting Information). No perturbations are observed in helices II or III, whereas modest $\Delta\omega_{NH}$ perturbations of 0.04−0.05 ppm are seen for the peaks of Lys10, Glu11, and Gly25 at 1.3-fold excess of ATPase domain. The progressively bigger shifts of the peaks of these residues upon successive additions of Hsc70 ATPase domain indicate the fast exchange regime and faster off-rate in 5 mM ATP. These observations in ATP suggest clearly weaker interaction of PyJ with the ATPase domain of Hsc70, but

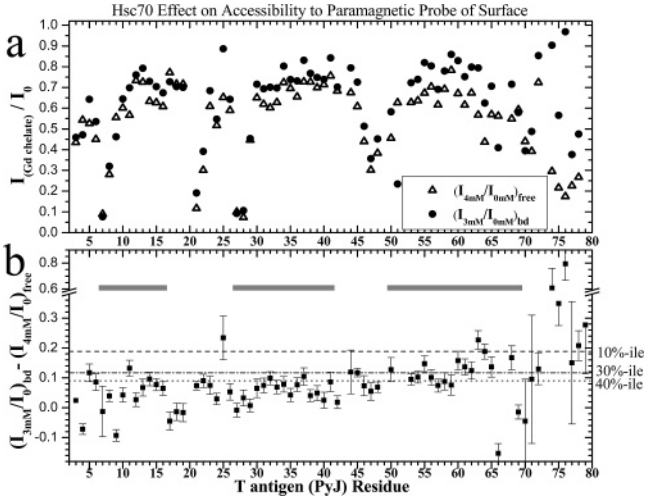

FIGURE 2: Effect of the Hsc70 ATPase domain on accessibility of PyJ to the global paramagnetic probe of the surface. In (a), the influence of the probe on peak heights of free PyJ is shown in open triangles and on Hsc70-saturated PyJ in filled circles. The peak heights when exposed to the line broadening agent Gd(DTPA-BMA) are normalized by their heights in the absence of the agent. The ratio of the Hsc70 ATPase domain to PyJ is 1.3. The slower tumbling of the complex results in greater line broadening per equivalent of paramagnetic probe (*32*). Consequently, the free state of ^{15}N PyJ probed with 4 mM gives similar broadening in nonaffected regions of the Hsc70-saturated state probed with 3 mM. In (b), the difference of the normalized peak heights for free and bound states from (a) is plotted. In (b), the 10 percentile most protected residues are bounded by the dashed line, the 30% percentile most protected by the dash−dotted line, and the 40 percentile most protected by the dotted line. Apart from additions of Gd(DTPA-BMA), ^{15}N TROSY spectra were collected under the conditions of Figure 1. Identical spectral parameters enabled quantitative comparison.

with Asp44 still interacting with the ATPase domain. This is consistent with the requirement of this conserved aspartate for stimulating ATPase activity. The dependence on ADP for greater overall interaction of PyJ with the ATPase domain agrees with expectations for a functional interaction that favors ATP hydrolysis.

With ADP present, the prominent participation of PyJ helix III in the interaction with the Hsc70 ATPase domain with ADP bound contrasts earlier NMR evidence that helix II of *E. coli* DnaJ is more important in its interaction with DnaK (*12*). Consequently, we sought to compare the chemical shift perturbation of PyJ by Hsc70 with complementary NMR methods.

Peak Broadening by Hsc70 Maps to Helix III of PyJ. At an interface in a large protein complex, line broadening can exceed the average broadening (*34*). Using spectra similar to those of Figure 1a, relative broadening among residues was compared by dividing amide peak heights of Hsc70-bound PyJ by peak heights of free PyJ. The peaks of PyJ most broadened in the complex with Hsc70 ATPase are from Gln32, Leu51, Met52, Glu65, Tyr67* (*quantification impaired by overlap), and most residues from Arg70 to Gln79 (Figure 1b). Leu16, Gly60, Thr64, Val66, and Thr76 are subtly broadened in the complex (Figure 1b). The line broadening is less than expected from the formation of a rigid 52.4 kDa complex. This suggests that PyJ might rock back and forth when associated with the nucleotide-binding domain.

Protection of the PyJ Surface from the Paramagnetic Probe by Hsc70. Cases are known where NMR peak positions are perturbed by binding-linked conformational changes outside the interface (*32*, *33*). This motivated us to apply a more accurate NMR mapping approach. That is, we measured the surface of PyJ protected by the Hsc70 ATPase domain from a paramagnetic agent (*32*, *35*). This is illustrated schematically in Figure S1 of Supporting Information. Gd-(DTPA-BMA) is recommended for probing protein surfaces because its inert, uncharged character makes it an excellent, nonselective global probe of the surface (*36*). Gd(DTPA-BMA) broadens ^{1}H NMR lines more on exposed surfaces of the macromolecule where the Gd(III) chelate approaches or collides. Sites the nucleotide-binding domain protects from the line broadening from the chelated Gd(III) probe are identified from the difference between the normalized peak heights of the free and Hsc70-saturated states of PyJ.

The surface accessibility of the backbone of PyJ is seen by mapping the broadening effects of the chelated Gd(III) probe onto the structure of PyJ (*18*). The high exposure of the termini, loops, and N-terminal ends of helices I and III is readily apparent from a drop in peak height in the presence of the paramagnetic probe (Figure 2a, open triangles). Periodicity in the surface accessibility of the backbone of all three helices is evident as a subtle rise and fall of peak broadening parameter $I_{Gd\ chelate}/I_0$ at the helical repeat of about 3.6 residues per turn of helix. In the middle of helix I, residues 11 and 14 are most exposed (Figure 2a, open triangles). In helix II, residues 32 and 36 are most exposed. In helix III, interior residues 53, 57, 61, 63, and 64 are most exposed. These measurements agree with the trends in main chain surface accessibility evident from the PDB coordinates (1FAF). Detection of the subtle helical periodicity builds confidence in the accuracy of the assay and the precision of these measurements on PyJ.

With that confidence, we compared the exposure of ^{15}N PyJ in its free state and saturated with Hsc70's ATPase domain (at pH 7.2 in ADP). The ATPase domain protects PyJ from Gd(DTPA-BMA) with a trend that increases from the N- to C-terminus of PyJ (Figure 2b). Helix II averages slightly higher Hsc70-dependent protection (0.06 ± 0.03) than helix I (0.04 ± 0.06). Helix III averages noticeably higher protection (0.13 ± 0.05 for residues 53−65) than helix II. Half of the residues of helix III are among the 30 percentile of residues most protected by Hsc70 (Figure 2b). Noteworthy is that these nine residues of helix III are protected by the ATPase domain as much as or more than conserved Asp44 of the HPD motif (Figure 2b). Also protected by Hsc70 are Gly25 and Asn72, Gly74 and Gly76 to Gln79 of the flexible C-terminal linker. Two turns in the middle of helix II are moderately protected, particularly Gln32 and Gln37. The paramagnetic protection corroborates the other NMR data that map the interface with the nucleotide-binding domain of Hsc70. It extends the view of the interface to include more of helix III and perhaps the center of helix II of PyJ.

Comparison of NMR Results on Hsc70-Binding Surfaces. Figure 3 shows the sites of PyJ most affected by the nucleotide-binding domain in the three NMR assays (Figures 1 and 2). The largest Hsc70-induced shifts of amide peaks map to the bend in helix III from Thr61 to Glu65, particularly Thr64 (Figure 3a). Similarly, the largest Hsc70-dependent

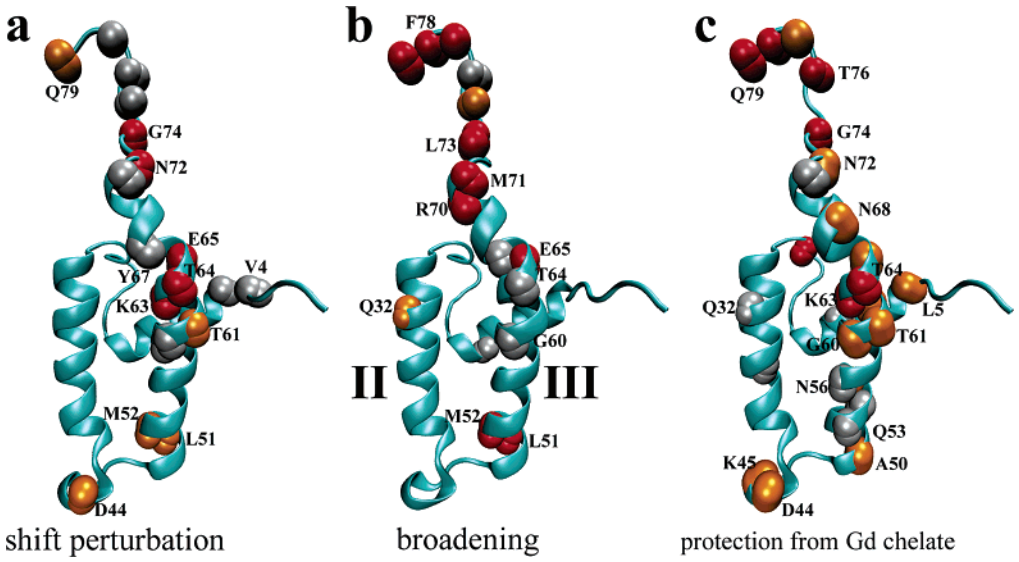

FIGURE 3: The nucleotide-binding domain of Hsc70 most affects helix III of PyJ by three NMR assays of the PyJ backbone. Backbone amide groups affected are marked upon the NMR structure of PyJ (*18*) (PDB accession code 1FAF, model 12), with spheres representing both amide proton and nitrogen. In panel a, red spheres indicate the Hsc70-binding-induced peak shifts $\Delta\omega_{HN}$ that rank among the 6% largest in Figure 1a, orange spheres those with $\Delta\omega_{HN}$ ranking from 6th to 13th percentile most shifted, and gray spheres those ranking from 13th to 26th percentile in peak shifts. In panel b, red spheres indicate the most Hsc70-decreased amide peaks with the lowest 10 percentile I_{bound}/I_{free} values of Figure 1b, orange spheres those with 10−16th percentile lowest I_{bound}/I_{free} of Figure 1b, and gray spheres ranking 16−20th percentile most decreased in the presence of Hsc70. In panel c, red spheres mark the 10% of the amide groups most protected by the ATPase domain from line broadening by the Gd(DTPA-BMA) cosolute, orange spheres the amide groups ranking 10−30th percentile most protected by Hsc70 from the probe, and gray spheres the amide groups ranking 30−40th percentile in protection from the probe.

protection of the folded region from line broadening by Gd(DTPA-BMA) (Figure 2) occurs in the bend of helix III, particularly at Lys63 and Thr64 (Figure 3c). Hsc70-dependent line broadening also maps to the bend of helix III (Figure 3b). On the basis of the peak shifts (Figure 3a) and the trusted protection from the Gd(DTPA-BMA) probe, Thr64 and Lys63 are hypothesized to be a "hot spot" of T antigen interaction with Hsc70. This is tested and supported by mutagenesis described below.

Gln32 and Gln37 of helix II are modestly protected from the paramagnetic probe by the ATPase domain (Figure 2b). They adjoin the bend in helix II (Figure 3c). Gln32 also experiences weak broadening and perhaps shifting of its backbone amide peak (Figures 1−3). Otherwise, the effects on helix II are surprisingly subtle.

At essential and exposed Asp44, the Hsc70-dependent peak shifts and protection from paramagnetic probe are smaller than the effects on the bend in helix III (Figures 1a and 2). This suggests Asp44 remains exposed on one side while docked to its site on the ATPase domain. Near the conserved HPD motif, the first turn of helix III is also affected by addition of the Hsc70 ATPase domain, displaying shifts and broadening of the backbone peaks of Leu51 and Met52 (Figure 3a,b). Both the first and second turns of helix III are modestly protected by Hsc70 from the paramagnetic probe (Ala50 and Gln53 through Asn56 in Figure 3c). This suggests the first two turns of helix III to be partly occluded in the interface with the ATPase domain but with shallower burial than at the bend in helix III (third, fourth, and fifth turns of the helix).

Evidence for Hsc70-Induced Conformational Adjustment of PyJ. C-Terminal linker residues 71 onward are significantly affected by the Hsc70 ATPase domain in all three NMR assays (Figure 3). The C-terminal linker of PyJ is highly mobile on picosecond−nanosecond time scales in the free state (*55*). The relatively large broadening of the peaks of the linker in the presence of the ATPase domain could be explained by the mobile linker becoming more restricted, with multiple conformations exchanging on the microsecond to millisecond time scale. A fluctuating ensemble of linker structures lying on the surface of the ATPase domain would also account for the peak shifts of the linker (Figure 3a) and for increased protection of residues 72−79 from collisions with Gd(DTPA-BMA) (Figures 2b and 3c). This behavior could be an artifact of use of the T antigen fragment lacking the loop structure present in full-length T antigen. Thus, we omit the C-terminal linker from the physiological Hsc70 interface that we propose to include helix III, HPD loop, and perhaps the center of helix II of PyJ (Figure 3).

Other Hsc70-affected residues in the NMR assays (background in Figure 3) are found especially at the N-terminus, helix I, and the I−II loop. Neighboring amide groups of Leu5 and Phe62, plus Glu11 and Leu14 of helix I and Gly25, are protected by the Hsc70 ATPase domain from the paramagnetic probe (Figures 2b and 3c). Val4, Asp9, and Val66 seem instead to be a little more exposed to the probe in the presence of the nucleotide-binding domain (Figure 2b). Movement of the N-terminus away from helix III of PyJ when bound to Hsc70 could potentially explain this. Hsc70-induced shifts of peaks of residues 4, 5, and 25 and broadening of Leu16 also map to this region. These observations suggest potential packing adjustments of the N-terminus, helix I, and I−II loop of PyJ in response to binding of the Hsc70 ATPase domain.

Hsc70-Protected Residues Map to the Solvent-Accessible Surface of the T Antigen Fragment Bound to pRb. The PyJ residues most protected by the Hsc70 ATPase domain from paramagnetic Gd(DTPA-BMA) (Figures 2 and 3c) may constitute the most reliable and accurate summary of the interface. These protected amides are marked on the ho-

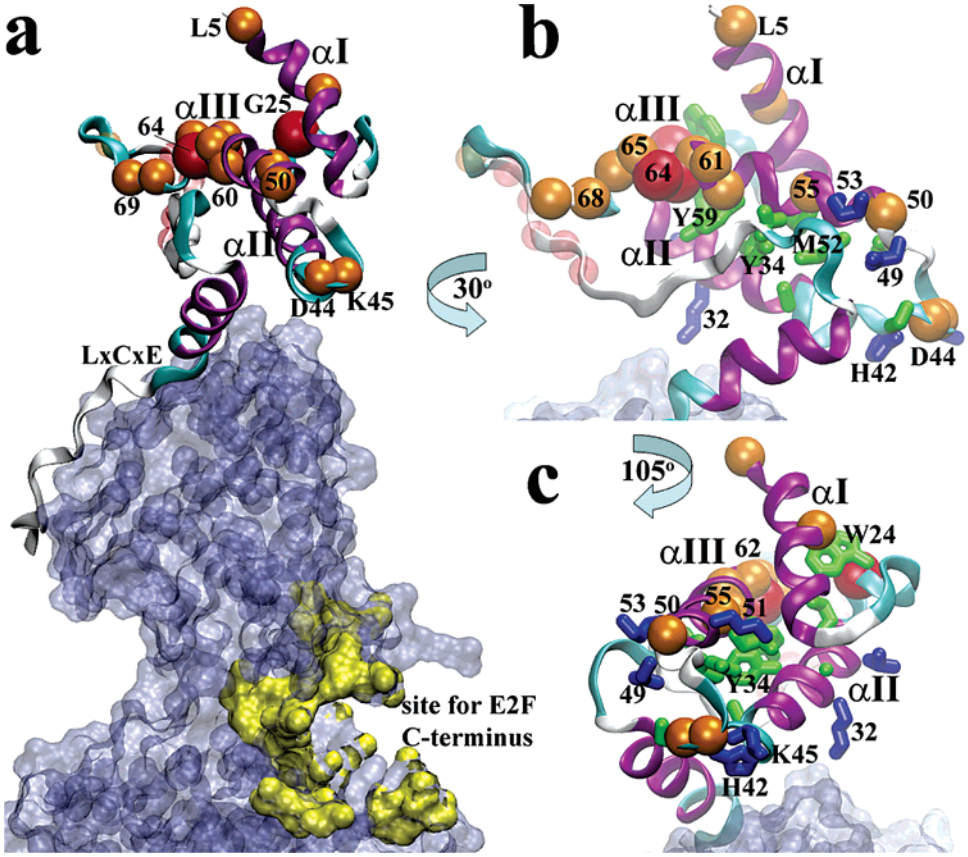

FIGURE 4: Hsc70-protected T antigen J domain residues map to a solvent-exposed surface of the crystal structure of the N-terminal fragment of SV40 T antigen (NT) bound to the pocket domain of pRb. NT residues 4−117 are represented with a ribbon using PDB coordinates 1GH6 (*8*). The pocket domain of pRb is represented with a blue, transparent molecular surface. As in Figure 3c, red spheres mark the 10th percentile of T antigen J domain backbone NH groups most protected by Hsc70 from paramagnetic probe. Orange spheres mark the 10−30th percentile next most protected sites. Protected amide groups of the linker that follows helix III are marked with smaller, transparent spheres since their structure differs in this larger assembly. Residue numbering includes letter labels for residues conserved between SV40 and murine polyomavirus. In panel a, the site of binding of E2F C-terminal residues 409−427 (*52*, *79*) is colored yellow on the far side of the pRb surface. In the zoomed and rotated views of the J domain in panels b and c, side chains are drawn where loss-of-function mutations were identified (*21*, *22*). Green indicates mostly buried side chains while blue indicates surface-accessible side chains.

mologous residues of the SV40 large T antigen J domain in the crystal structure of its N-terminal fragment (NT) bound to the pRb pocket domain (red and orange spheres in Figure 4). Much of helix II (except for residues 29, 36, 37, and 40) is buried in this crystal structure. The J domain residues most protected by Hsc70 map to a readily accessible surface in the complex of NT with pRb (Figure 4). The correspondence between exposure in the NT/pRB complex and sites of apparent Hsc70 contact is striking. An Hsc70 binding interface centered upon helix III and conserved Asp44 of T antigen may explain how Hsc70 can bind pRb-bound T antigen, despite apparent inaccessibility of helix II (Figure 4). Hsc70 docking to helix III of T antigen's J domain can be hypothesized to place the substrate-binding domain of Hsc70 near an E2F bound to pRb; see the cleft in pRb where the C-termini of E2Fs are known to bind (yellow in Figure 4a).

pRb-Binding Region of E2F1 Is Unfolded and a Substrate of Hsc70 in Vitro. The region of human E2F1 that binds pRb avidly extends from its marked box region to the C-terminus, i.e., from about residue 243 through 437 (*52*). The unfolded E2F1 fragment from residues 200 through 301 was recently shown to adopt structure upon forming its heterodimer with DP1 (*56*). ^{15}N HSQC spectra of E2F1 (aa 243−437), albeit in the absence of DP1, have peaks with predominantly random coil chemical shifts (Figure 5) at 20−30 °C, indicating that it is mostly unfolded. One hundred thirty-seven backbone amide peaks among 174 possible are observed in the E2F1 (aa 243−437) spectra. The 21% of possible peaks missing are likely either broadened beyond detection or overlapped. Broadening from exchange between conformational substates is found in unfolded or disordered proteins. Sequence-based predictors of natural disordered regions (PONDR) (*57*−*59*) strongly predict inherent disorder in residues 300 through 365 of E2F1 (Figure S3 of Supporting Information). This prediction and the NMR observation of disorder throughout free E2F1 (aa 243−437) (Figure 5) suggest that disorder of residues beyond 300 may persist while DP1 is bound to E2F1 residues 200−300.

Unfolded proteins and peptides are known to serve as substrates of Hsc70 (*60*, *61*). Peptide substrates are known to increase the velocity of the ATPase activity of the hsp70 DnaK (*62*) We tested whether human Hsc70 could act on human E2F1 (aa 243−437) as substrate and whether T antigens might have the capacity to stimulate this. To do so, we tested whether human E2F1 (aa 243−437) and PyJ stimulate the ATPase activity of human Hsc70. We monitored ATP hydrolysis via the formation of inorganic phosphate (P_i) detected by an indicator dye (*50*, *51*). Neither Hsc70 alone nor the E2F1 fragment alone enhances ATP

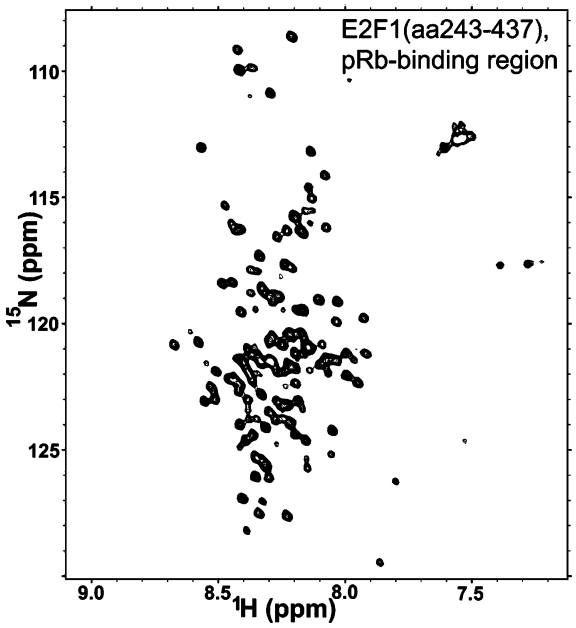

FIGURE 5: ^{15}N HSQC of the avid pRb-binding region of human E2F1 (aa 243−437) (*52*). The amide peaks in the spectrum lie mainly at random coil chemical shifts. The 1.9 mM protein was studied at 20 °C in 150 mM NaCl and 20 mM sodium phosphate, pH 6.5.

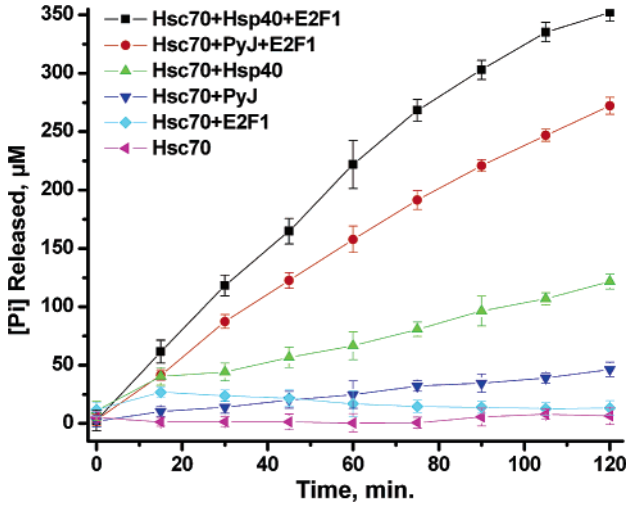

FIGURE 6: Human E2F1 (aa 243−437) is a substrate of human Hsc70 in vitro, stimulating the ATPase activity in a PyJ- or HDJ-1-dependent manner. Concentrations used in the 50 μL chaperone reaction volume at 40 °C were 635 μM ATP, 290 nM full-length Hsc70, 800 nM E2F1(aa 243−437), 2 μM PyJ, and 490 nM full-length HDJ-1. ATP hydrolysis was detected colorimetrically as the formation of P_i in a buffer containing malachite green, ammonium molybdate, and nonionic detergent (*50*, *51*). [P_i] was estimated from the equivalence of $1A_{660nm}$ (1 cm path length, detected in 950 μL) to 495 μM P_i in the chaperone reaction volume of 50 μL, based on KH_2PO_4 standards. Nonenzymatic background P_i formation from spontaneous ATP hydrolysis was subtracted. The measurements were done in triplicate, providing the uncertainties.

hydrolysis. Addition of E2F1 (aa 243−437) modestly increases Hsc70 ATPase activity initially without subsequent turnover (Figures 6 and 7). Addition of PyJ stimulates Hsc70 to hydrolyze ATP with continuing turnover, to a moderate extent similar to a previous report (*63*). When *both* E2F1 (aa 243−437) and PyJ are added to Hsc70, ATP is hydrolyzed about 6-fold faster than in the absence of E2F1 (Figure 6). Addition of human Hsp40 to Hsc70 stimulates

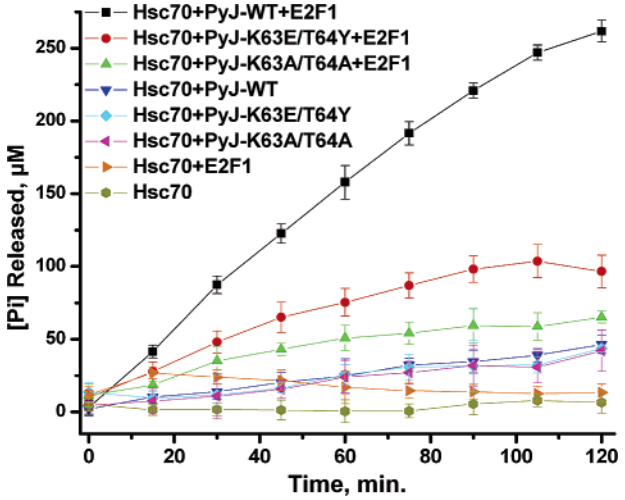

FIGURE 7: Double mutations of Lys63 and Thr64 impair PyJ stimulation of substrate-dependent Hsc70 ATPase activity. The conditions and concentrations are the same as for Figure 6. Use of K63E/T64Y and K63A/T64A double mutants is indicated in the legend.

ATP hydrolysis by human Hsc70 more than does addition of PyJ, whether E2F1 is present or not (Figure 6). Greater stimulation of human Hsc70 by human Hsp40 than by the PyJ fragment of T antigens may be attributable to better species match and the full length of Hsp40. When Hsc70 is stimulated by addition of E2F1 (aa 243−437) and a cochaperone, most of the ATP available is hydrolyzed in 2 h at 40 °C: about 95% in the case of the Hsp40 cochaperone and about 73% with the PyJ cochaperone. The results are consistent with the hypothesis that E2F1 could be a substrate of Hsc70 recruited by large T antigen to pRb in vivo.

Contribution of Lys63 and Thr64 of T Antigen to Hsc70 Stimulation. Using the new assay of Hsc70 with the E2F1 fragment as substrate, we sought to test the functional importance of PyJ residues Lys63 and Thr64 found by NMR to interact with Hsc70 (Figures 1−3). Two different double mutations of this pair of surface residues were prepared: K63E/T64Y and K63A/T64A. The assay's conditions of 7-fold excess of PyJ over Hsc70 should foster their interaction if impaired by mutation. In the absence of protein substrate for Hsc70, each double mutant of PyJ was only slightly below wild-type PyJ in enhancing the ATPase rate modestly (Figure 7). However, both double mutants are markedly diminished in ability to stimulate high ATPase activity of Hsc70 working on the unfolded protein substrate E2F1 (aa 243−437). Under the conditions with E2F1 substrate, K63E/T64Y stimulates 36% of wild-type ATPase activity and K63A/T64A stimulates 21% of wild-type ATPase activity (Figure 7). The side chain truncation of the latter mutant evidently is more deleterious. The mutational interference suggests the relevance of these residues to catalytic turnover and the NMR mapping performed by necessity under nonturnover, equilibrium conditions.

Evolutionary Trace Analysis of J Domains. We sought to assess the relevance of the NMR-based mapping of PyJ to the features that J domains in general use for hsp70 recognition, other than the conserved HPD motif. So we conducted evolutionary trace analysis (ET) of the J domain superfamily. References *38* and *42* introduce the ET method. In short, ET finds residue positions characteristic of protein

subfamilies, i.e., class-specific residues expected to confer specificity and to cluster with conserved residues at functional sites.

Multiple sequence alignment divided a refined set of J domain sequences into three subgroups of 499, 199, and 81 members, respectively. The largest group includes orthodox, archetypal J domains of *E. coli* DnaJ and human Hsp40 (HDJ-1) that are type I and type II J domains, respectively. Representative viral J domain sequences (type III J domains), among them PyJ, belong to the 199-member second major subgroup sharing homology with the viral J domains. These two major subgroups have members with NMR or X-ray structures available for use in the structural mapping step of ET. Since the divergent third subgroup lacks an experimental structure for use in ET, this small subgroup was dropped from consideration. At the seventh trace (sequence identity) level, where sequence identities are ~70% or higher within subfamilies of J domains, the phylogenetic tree of the 499-member group partitions into 94 subfamilies and that of the 199-member group into 34 subfamilies. The consensus sequences (conserved positions) within each of these subfamilies are shown with the class-specific positions characteristic of subfamilies indicated (Figures S4 and S5 of Supporting Information). "Subgroup analysis" (*42*) was performed to predict what positions are important to the specificity of the superfamily of J domains as a whole. That is, the intersection of the class-specific residues from the larger and smaller major groups was taken to identify positions that tune specificity in both subgroups. The largest group is represented by the NMR structure of the J domain of either human Hsp40 (HDJ-1) shown here (*64*) or similar *E. coli* DnaJ (*65*). The second principal group is represented by the NMR structure of PyJ from polyomavirus T antigens (*18*). The class-specific residues of the larger subgroup in the numbering of human Hsp40 are Asp3, Tyr5, Leu8, Gly9, Lys20, Tyr23, Arg24, Ala27, Leu28, Asp33, Phe44, Lys45, Ala50, Tyr51, Leu54, Asp56, Lys59, Phe63, Asp64, and Gly67 (Figure S4 in Supporting Information). The class-specific residues of the smaller subgroup in PyJ numbering are Leu13, Leu14, Leu17, Met30, Gln31, Tyr34, Lys35, Gln37, Ser38, Leu39, Leu41, Met52, Leu55, Leu58, Trp59, Phe62, Thr64, and Asn68 (Figure S5 in Supporting Information). The underlined residues are class-specific positions shared by *both* major subgroups of J domains and are colored red on the structures of HDJ-1 and PyJ in Figure 8. (The alignment is the structure-aided alignment of ref *18*). These shared class-specific residues can be hypothesized to tune the specificity of both principal subgroups of J domains. Buried residues among these may be important for adjusting the packing that underlies hsp70 interaction surfaces. The shared class-specific residues include five that are contiguous on the surface of helix II and five positions on helix III. The latter lie on the first, fourth, and fifth turns of helix III in the a1′, g1′, a2′, d2′, and f2′ positions, using coiled-coil heptad repeat nomenclature (*18*). The a1′, a2′, g1′, and d2′ positions are buried and must support the structure (*18*). The side chains of Met52, Trp59, and Thr64 of PyJ (a1′, a2′, and f2′ positions) cluster together with the five class-specific residues of the helix II surface (Figure 8). The residues that are class-specific within only one of the major groups of J domains appear on the periphery (pink in Figure 8). In the largest group of J domains, four of these class-specific residues notably encompass the QKRAA motif reported to be important in bacterial J domains (*23*, *26*) (pink at top of Figure 8a). The residues of helices II and III that are class-specific in both major subgroups of J domains (red in Figure 8), combined with the conserved HPD motif, may be hypothesized to support hsp70 recognition by most J domains.

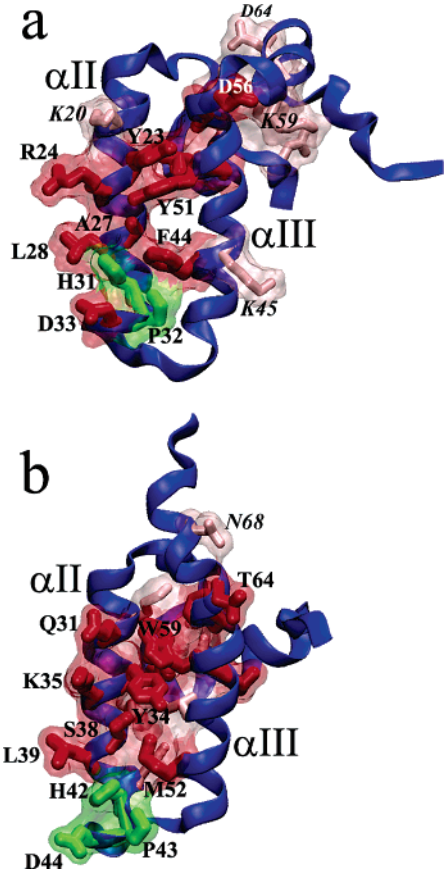

FIGURE 8: Residues predicted to influence hsp70 recognition, i.e., class-specific residues from evolutionary trace analysis, map not only to helix II but also to helix III and the C-terminal end of J domains. Panel a represents the largest subgroup of J domains with the NMR structure of HDJ-1 (human Hsp40) (*64*) (PDB accession code 1HDJ). Panel b represents the second major group of J domains with the NMR structure of PyJ from T antigens (*18*) (PDB accession code 1FAF). Panel a used the largest subgroup of 499 J domain sequences that partitioned into 94 subfamilies at the seventh trace level, corresponding to sequence identities above 72% within subfamilies. Panel b used the smaller principal subgroup of J domains, comprising 199 sequences. These partitioned into 34 subfamilies at the seventh trace level, corresponding to sequence identities above 67% within subfamilies. The surfaces of conserved and class-specific residues are plotted. Conserved residues of the HPD motif are shown with side chains in green. Class-specific residues common to both major subgroups are drawn with red side chains. Residues that are class-specific only within that major subgroup are drawn with thinner side chains in pink. These residues on the proximal surfaces are labeled.

DISCUSSION

NMR and Mutagenesis Evidence That Helix III of the Viral J Domain Interacts with Hsc70. We initially expected that helix II of PyJ (T antigen) would be central to its interface with the Hsc70 ATPase domain as reported for the *E. coli* DnaJ interface with DnaK (*12*). However, all three NMR

assays of PyJ agree in suggesting a much greater role for helix III of T antigens in Hsc70 recognition, particularly around the bend near the C-terminal end of helix III (Figure 3). We especially trust the accuracy of the mapping of Hsc70 protection of PyJ from the paramagnetic agent (Figures 2 and 3c). A role for helix III of T antigens in Hsc70 recognition was suggested recently by loss-of-function mutations at Lys51, Lys53, Met55, Asn56, and Tyr59 of SV40 (*21*) and at His49, Met52, and Asn56 of murine polyomavirus (*22*). Six of these seven important surface residues agree with and supplement the Hsc70 contacts identified by NMR (Figure 4b,c). K63R or T64S substitutions of polyomavirus T antigen failed to disrupt pRb- and E2F-dependent transactivation (*22*); this could be attributed to how minimal is the alteration of the chemical properties by such conservative mutations. By contrast, the K63A/T64A or K63E/T64Y double mutants suffice to impair substrate-dependent Hsc70 stimulation (Figure 7); we designed them for more disruptive size and charge alterations. Our results extend the view of the interface to include the bend region of helix III and suggest the NMR mapping is relevant to the interactions during catalysis.

Many essential side chains identified by mutagenesis of T antigens (*21, 22, 66*−*68*) are buried in or near the core of the J domain (*18*) or within the larger NT fragment bound to the pRb pocket domain (green in Figure 4b,c). The lesions at the buried sites are likely to disrupt actual Hsc70 interaction surfaces nearby. Conservative substitutions in the core may cause enough disruption to propagate to the recognition surface, but without destabilizing the T antigen so much that it is lost to proteolytic turnover. Evolutionary trace analysis also supports the importance of the core residues between the helices (Figure 8), again implying their long-range connection to hsp70 interaction by shaping the recognition surface.

Surface of Hsc70 Recognition in the T Antigen Complex with pRb. The greater role proposed for helix III largely resolves the dilemma stemming from our initial hypothesis that helix II of the J domain would be the main site of interaction with Hsc70 outside the conserved HPD motif. The chaperone hypothesis requires that Hsc70 bind a complex of pRb, large T antigen, and presumably E2F (*7, 8*). In the crystal structure of pRb bound to the NT fragment of SV40 large T antigen, helix II of the J domain packs with other portions of NT and pRb (*8*). Helix II is obstructed on one side by close approach of pRb and another side by the loop and helix IV connecting the J domain with the Rb recognition element (LxCxE motif) of large T antigen (*14*) (Figure 4). The dilemma of steric hindrance to helix II seems to be largely resolved by the importance of helix III of the J domain in recognizing Hsc70. The sites of Hsc70 contact in helix III and the HPD loop (Figure 3) all map to surfaces readily accessible in the structure of the NT/pRb complex (Figure 4). The interface mapping data presented in this work are qualitatively consistent with the hypothesis that the broad surface across helices II and III faces Hsc70; this concept is implied by the computational model of the auxilin J domain docked to Hsc70 (1Q2G) (*69*). Yet the authors of the model noted the steric hindrance to Hsc70 access to the helix II portion of this surface of T antigen bound to pRb, unless relieved by rearrangement of the linker within T antigen (*14*). Our data suggest the need for a rotation in docking orientation, such that Hsc70 approaches T antigen's helix III much more intimately and helix II much less, if at all.

Helix II. The subtle NMR effects (Figures 1−3), mutagenesis, and ET suggest that helix II of viral J domains still may contribute to interaction with Hsc70. There are potential scenarios where helix II might participate: (i) It is conceivable that helix II has contacts with full-length hsp70 at a region outside the nucleotide-binding domain. (ii) It is also possible that side chains of helix II of PyJ (candidates being Gln32, Lys35, and Gln37) contact the ATPase domain of Hsc70. The subtlety of spectral effects on the backbone of helix II might be consistent with side chains of helix II interacting with Hsc70 at the *edge* of their interface. If helix II plays either of roles i or ii, the question of relative inaccessibility to Hsc70 of helix II of the NT fragment of T antigen bound to the pRb pocket domain returns (Figure 4). Contact of Hsc70 with the tentative sites on helix II (weakly affected in Figures 1−3) in the complex would require unburial of helix II, possibly by displacement of the linker joining helices III and IV (Figure 4b). High *B*-factors of linker residues 77−97 in the X-ray coordinates [1GH6 (*8*)] and low order parameters of the linker residues 70−79 (*70*) suggest the linker's flexibility might allow its displacement from helix II, as previously postulated (*14*). The pRb-binding (NT) fragment of murine polyomavirus large T antigen is 260 residues and much longer than SV40 NT. In the former, the degree of burial of helix II is unknown.

Comparison with Bacterial and Other hsp70/J Domain Interactions. *E. coli* DnaK also affects NMR peaks of helix III residues of DnaJ, namely, Phe47, Tyr54, and Thr58 (*12, 20*). These residues of *E. coli* DnaJ helix III align in sequence with Hsc70-affected residues of PyJ (Figures 1−3); see the alignment in ref *18*. ET of J domains suggests that helix III and the C-terminal end of a J domain may often accompany helix II in hsp70 recognition (Figure 8). In orthodox (type I and II) J domains, ET strengthens previous data on hsp70 recognition by bacterial J domains (*23*−*27*), in suggesting participation of the C-terminal end of helix III, the loop joining helices III and IV, and helix IV corresponding to the QKRAA motif. That region roughly corresponds to the Hsc70 recognition hot spot in the bend of helix III of PyJ (Figures 3 and 7). ET suggests that these sites may join in tailoring specificity of J domains for their hsp70 partners in most organisms.

Our observations satisfactorily explain how the ternary complex of large T antigen, Rb family member, and Hsc70 can form without competition. Yet there remain striking differences of the PyJ−Hsc70 interaction from the DnaJ−DnaK interaction (*12*). The participation of helix III did become more evident in a more recent study of the DnaJ−DnaK interaction (*20*). The NMR evidence of PyJ helix II involvement in Hsc70 interaction (Figures 1−3) is much more subtle than the NMR results for *E. coli* DnaJ interaction with DnaK (*12, 20*). Perhaps DnaK's approach to DnaJ could be oriented more toward helix II while Hsc70's approach to viral J domains could be oriented more toward helix III. PyJ harbors only one of the usual four positively charged residues in the midsection of helix II of J domains (*18*); could this account for less intimate contact of PyJ helix II with Hsc70? Not only does the implied contact interface differ, but the kinetic regime differs as well. The kinetics of the interaction of DnaJ and DnaK is fast on the NMR time scale, whereas

that of PyJ with the Hsc70 ATPase domain is slow on the NMR time scale. Slow kinetics were also observed for the interaction of PyJ with the Hsc70 ATPase domain when monitored by the chemical shift changes of the ATPase domain (Y. Zhang and E. Zuiderweg, unpublished results). This divergent, viral J domain may have mechanistic features that are genuinely distinctive from orthodox J domains. Indeed, chimeric T antigens using a J domain from yeast Ydj-1 or *E. coli* DnaJ failed to support DNA replication or transformation in mammalian host cells (*44*).

On Hsc70, pRb, E2Fs, and Disassembly. The chaperone hypothesis (*7*, *8*) coupled with data presented above suggests the following revised question: Does large T antigen bound to an Rb family member position Hsc70's substrate binding domain into *direct* contact with an E2F bound to the Rb family member? The evidence that the Rb-binding region of human E2F1 (aa 243−437) may have a disordered region that could persist after DP1 binding raises the question of whether it is a pathophysiological substrate of Hsc70. The observation that E2F1 (aa 243−437) stimulates ATP hydrolysis by Hsc70 in a manner strongly dependent on PyJ or on Hsp40 indicates that E2F1 is a substrate at least in vitro. The assay suggests the possibility of catalytic action of Hsc70 upon E2F present in a quaternary complex of Hsc70, T antigen, Rb family member, and E2F. It is conceivable that the chaperone activity and ATP hydrolysis may provide favorable free energy for releasing the E2F from the Rb family member.

The efficiency of pRb-independent activation of the cyclin A promoter (*71*) was recently shown to be impaired by the same large T antigen helix II and III mutations (of residues 32, 33, 34, 49, 52, or 56) that impair pRb- and E2F-dependent transactivation (*22*). Thus, transactivation of the cyclin A promoter by the reported assembly of transcription factors and large T antigen (*72*) could depend on Hsc70 recruited there by T antigen. Might large T antigen recruit Hsc70 to still other assemblies of transcription factors it joins, such as TBP-associated factors (*73*, *74*)? By analogy with E2F1, could disordered segments of other transcription factors render them susceptible to Hsc70?

We have provided the first unambiguous evidence that the third helix of a J domain, that of T antigens, plays an important role in hsp70 interaction. Our evidence clarifying a hypothesis of T antigen-recruited, Hsc70-catalyzed release of an E2F family member from an Rb family member (Figures 5 and 6) extends previous descriptions of hsp70-catalyzed disassembly processes. *E. coli* DnaK, together with DnaJ and GrpE, was shown to help to disassemble protein components of the replication initiation complex, separating RepA into monomers, in the course of phage λ replication in *E. coli* (*75*−*78*). Large T antigen and its N-terminal fragment (NT) were shown to release unfolded polypeptides bound to the yeast hsp70 known as Ssa1p (*7*). Pathophysiologically relevant E2F1 and other E2Fs are now hypothesized to be potential *substrates* of Hsc70 recruited by large T antigen.

ACKNOWLEDGMENT

We are grateful to D. McKay for the expression vector for the bovine Hsc70 ATPase domain and to B. Xiao and S. Gamblin for the expression vector for GST-E2F1 (aa 243−437; human). We thank the MRI clinic of the University of Missouri Hospital for the gift of Omniscan, i.e., Gd(DTPA-BMA). We are grateful to M. Berjanskii for critically reading the manuscript and to W. Folk for comments. We thank Y. Zhang and V. Semenchenko for technical tips on handling the nucleotide-binding domain of Hsc70.

SUPPORTING INFORMATION AVAILABLE

Figure S1 providing a schematic illustration of mapping a biomolecular interface by exclusion of paramagnetic, chelated Gd(III), Figure S2 reporting on a negative control titration of the Hsc70 nucleotide-binding domain into PyJ in the presence of ATP, Figure S3 showing a PONDR prediction of disorder in the sequence of human E2F1, Figure S4 displaying the consensus sequences of the subfamilies of the largest group of J domains and the residues distinguishing the subfamilies, and Figure S5 providing the consensus sequences of the subfamilies of the second largest group of J domains and the residues distinguishing the subfamilies. This material is available free of charge via the Internet at http://pubs.acs.org.

REFERENCES

1. Harbour, J. W., and Dean, D. C. (2000) The Rb/E2F pathway: expanding roles and emerging paradigms, *Genes Dev. 14*, 2393−2409.
2. Nevins, J. R. (2001) The Rb/E2F pathway and cancer, *Hum. Mol. Genet. 10*, 699−703.
3. Wu, L., Timmers, C., Maiti, B., Saavedra, H. I., Sang, L., Chong, G. T., Nuckolls, F., Giangrande, P., Wright, F. A., Field, S. J., Greenberg, M. E., Orkin, S., Nevins, J. R., Robinson, M. L., and Leone, G. (2001) The E2F1-3 transcription factors are essential for cellular proliferation, *Nature 414*, 457−462.
4. Frolov, M. V., and Dyson, N. J. (2004) Molecular mechanisms of E2F-dependent activation and pRB-mediated repression, *J. Cell. Sci. 117*, 2173−2181.
5. Vilchez, R. A., and Butel, J. S. (2004) Emergent human pathogen simian virus 40 and its role in cancer, *Clin. Microbiol. Rev. 17*, 495−508.
6. Brodsky, J. L., and Pipas, J. M. (1998) Polyomavirus T antigens: molecular chaperones for multiprotein complexes, *J. Virol. 72*, 5329−5334.
7. Srinivasan, A., McClellan, A. J., Vartikar, J., Marks, I., Cantalupo, P., Li, Y., Whyte, P., Rundell, K., Brodsky, J. L., and Pipas, J. M. (1997) The amino-terminal transforming region of simian virus 40 large T and small t antigens functions as a J domain, *Mol. Cell. Biol. 17*, 4761−4773.
8. Kim, H. Y., Ahn, B. Y., and Cho, Y. (2001) Structural basis for the inactivation of retinoblastoma tumor suppressor by SV40 large T antigen, *EMBO J. 20*, 295−304.
9. Sheng, Q., Denis, D., Ratnofsky, M., Roberts, T. M., DeCaprio, J. A., and Schaffhausen, B. (1997) The DnaJ domain of polyomavirus large T antigen is required to regulate Rb family tumor suppressor function, *J. Virol. 71*, 9410−9416.
10. Sullivan, C. S., Cantalupo, P., and Pipas, J. M. (2000) The molecular chaperone activity of simian virus 40 large T antigen is required to disrupt Rb-E2F family complexes by an ATP-dependent mechanism, *Mol. Cell. Biol. 20*, 6233−6243.
11. Campbell, K. S., Mullane, K. P., Aksoy, I. A., Stubdal, H., Zalvide, J., Pipas, J. M., Silver, P. A., Roberts, T. M., Schaffhausen, B. S., and DeCaprio, J. A. (1997) DnaJ/hsp40 chaperone domain of SV40 large T antigen promotes efficient viral DNA replication, *Genes Dev. 11*, 1098−1110.
12. Greene, M. K., Maskos, K., and Landry, S. J. (1998) Role of the J-domain in the cooperation of Hsp40 with Hsp70, *Proc. Natl. Acad. Sci. U.S.A. 95*, 6108−6113.
13. Walsh, P., Bursac, D., Law, Y. C., Cyr, D., and Lithgow, T. (2004) The J-protein family: modulating protein assembly, disassembly and translocation, *EMBO Rep. 5*, 567−571.
14. Gruschus, J. M., Han, C. J., Greener, T., Ferretti, J. A., Greene, L. E., and Eisenberg, E. (2004) Structure of the functional

fragment of auxilin required for catalytic uncoating of clathrin-coated vesicles, *Biochemistry 43*, 3111−3119.
15. Cheetham, M. E., and Caplan, A. J. (1998) Structure, function and evolution of DnaJ: conservation and adaptation of chaperone function, *Cell Stress Chaperones 3*, 28−36.
16. Wall, D., Zylicz, M., and Georgopoulos, C. (1994) The NH_2-terminal 108 amino acids of the *Escherichia coli* DnaJ protein stimulate the ATPase activity of DnaK and are sufficient for lambda replication, *J. Biol. Chem. 269*, 5446−5451.
17. Tsai, J., and Douglas, M. G. (1996) A conserved HPD sequence of the J-domain is necessary for YDJ1 stimulation of Hsp70 ATPase activity at a site distinct from substrate binding, *J. Biol. Chem. 271*, 9347−9354.
18. Berjanskii, M. V., Riley, M. I., Xie, A., Semenchenko, V., Folk, W. R., and Van Doren, S. R. (2000) NMR structure of the N-terminal J domain of polyomavirus T antigens: implications for DnaJ-like domains and for T antigen mutations, *J. Biol. Chem. 275*, 36094−36103.
19. Genevaux, P., Schwager, F., Georgopoulos, C., and Kelley, W. L. (2002) Scanning mutagenesis identifies amino acid residues essential for the in vivo activity of the *Escherichia coli* DnaJ (Hsp40) J-domain, *Genetics 162*, 1045−1053.
20. Landry, S. J. (2003) Structure and energetics of an allele-specific genetic interaction between dnaJ and dnaK: correlation of nuclear magnetic resonance chemical shift perturbations in the J-domain of Hsp40/DnaJ with binding affinity for the ATPase domain of Hsp70/DnaK, *Biochemistry 42*, 4926−4936.
21. Fewell, S. W., Pipas, J. M., and Brodsky, J. L. (2002) Mutagenesis of a functional chimeric gene in yeast identifies mutations in the simian virus 40 large T antigen J domain, *Proc. Natl. Acad. Sci. U.S.A. 99*, 2002−2007.
22. Whalen, K. A., de Jesus, R., Kean, J. A., and Schaffhausen, B. S. (2005) Genetic analysis of the polyomavirus DnaJ domain, *J. Virol. 79*, 9982−9990.
23. Auger, I., Escola, J. M., Gorvel, J. P., and Roudier, J. (1996) HLA-DR4 and HLA-DR10 motifs that carry susceptibility to rheumatoid arthritis bind 70-kD heat shock proteins, *Nat. Med. 2*, 306−310.
24. Auger, I., Lepecuchel, L., and Roudier, J. (2002) Interaction between heat-shock protein 73 and HLA-DRB1 alleles associated or not with rheumatoid arthritis, *Arthritis Rheum. 46*, 929−933.
25. Auger, I., and Roudier, J. (1997) A function for the QKRAA amino acid motif: mediating binding of DnaJ to DnaK. Implications for the association of rheumatoid arthritis with HLA-DR4, *J. Clin. Invest. 99*, 1818−1822.
26. Suh, W. C., Lu, C. Z., and Gross, C. A. (1999) Structural features required for the interaction of the Hsp70 molecular chaperone DnaK with its cochaperone DnaJ, *J. Biol. Chem. 274*, 30534−30539.
27. Hennessy, F., Boshoff, A., and Blatch, G. L. (2005) Rational mutagenesis of a 40 kDa heat shock protein from *Agrobacterium tumefaciens* identifies amino acid residues critical to its in vivo function, *Int. J. Biochem. Cell Biol. 37*, 177−191.
28. Hennessy, F., Nicoll, W. S., Zimmermann, R., Cheetham, M. E., and Blatch, G. L. (2005) Not all J domains are created equal: implications for the specificity of Hsp40-Hsp70 interactions, *Protein Sci. 14*, 1697−1709.
29. Takahashi, H., Nakanishi, T., Kami, K., Arata, Y., and Shimada, I. (2000) A novel NMR method for determining the interfaces of large protein-protein complexes, *Nat. Struct. Biol. 7*, 220−223.
30. Clore, G. M., and Schwieters, C. D. (2003) Docking of protein-protein complexes on the basis of highly ambiguous intermolecular distance restraints derived from $^{1}H/^{15}N$ chemical shift mapping and backbone ^{15}N-^{1}H residual dipolar couplings using conjoined rigid body/torsion angle dynamics, *J. Am. Chem. Soc. 125*, 2902−2912.
31. Pellecchia, M. (2005) Solution nuclear magnetic resonance spectroscopy techniques for probing intermolecular interactions, *Chem. Biol. 12*, 961−971.
32. Arumugam, S., Hemme, C. L., Yoshida, N., Suzuki, K., Nagase, H., Berjanskii, M., Wu, B., and Van Doren, S. R. (1998) TIMP-1 contact sites and perturbations of stromelysin 1 mapped by NMR and a paramagnetic surface probe, *Biochemistry 37*, 9650−9657.
33. Takeda, M., Terasawa, H., Sakakura, M., Yamaguchi, Y., Kajiwara, M., Kawashima, H., Miyasaka, M., and Shimada, I. (2003) Hyaluronan recognition mode of CD44 revealed by cross-saturation and chemical shift perturbation experiments, *J. Biol. Chem. 278*, 43550−43555.
34. Matsuo, H., Walters, K. J., Teruya, K., Tanaka, T., Gassner, G. T., Lippard, S. J., Kyogoku, Y., and Wagner, G. (1999) Identification by NMR spectroscopy of residues at contact surfaces in large, slowly exchanging macromolecular complexes, *J. Am. Chem. Soc. 121*, 9903−9904.
35. Arumugam, S., and Van Doren, S. R. (2003) Global orientation of bound MMP-3 and N-TIMP-1 via residual dipolar couplings, *Biochemistry 42*, 7950−7958.
36. Pintacuda, G., and Otting, G. (2002) Identification of protein surfaces by NMR measurements with a pramagnetic Gd(III) chelate, *J. Am. Chem. Soc. 124*, 372−373.
37. Gao, G., Prutzman, K. C., King, M. L., Scheswohl, D. M., DeRose, E. F., London, R. E., Schaller, M. D., and Campbell, S. L. (2004) NMR solution structure of the focal adhesion targeting domain of focal adhesion kinase in complex with a paxillin LD peptide: evidence for a two-site binding model, *J. Biol. Chem. 279*, 8441−8451.
38. Lichtarge, O., Bourne, H. R., and Cohen, F. E. (1996) An evolutionary trace method defines binding surfaces common to protein families, *J. Mol. Biol. 257*, 342−358.
39. Lichtarge, O., Bourne, H. R., and Cohen, F. E. (1996) Evolutionarily conserved Galphabetagamma binding surfaces support a model of the G protein-receptor complex, *Proc. Natl. Acad. Sci. U.S.A. 93*, 7507−7511.
40. Sowa, M. E., He, W., Slep, K. C., Kercher, M. A., Lichtarge, O., and Wensel, T. G. (2001) Prediction and confirmation of a site critical for effector regulation of RGS domain activity, *Nat. Struct. Biol. 8*, 234−237.
41. Madabushi, S., Yao, H., Marsh, M., Kristensen, D. M., Philippi, A., Sowa, M. E., and Lichtarge, O. (2002) Structural clusters of evolutionary trace residues are statistically significant and common in proteins, *J. Mol. Biol. 316*, 139−154.
42. Lichtarge, O., and Sowa, M. E. (2002) Evolutionary predictions of binding surfaces and interactions, *Curr. Opin. Struct. Biol. 12*, 21−27.
43. Cyr, D. M., and Douglas, M. G. (1994) Differential regulation of Hsp70 subfamilies by the eukaryotic DnaJ homologue YDJ1, *J. Biol. Chem. 269*, 9798−9804.
44. Sullivan, C. S., Tremblay, J. D., Fewell, S. W., Lewis, J. A., Brodsky, J. L., and Pipas, J. M. (2000) Species-specific elements in the large T-antigen J domain are required for cellular transformation and DNA replication by simian virus 40, *Mol. Cell. Biol. 20*, 5749−5757.
45. O'Brien, M. C., and McKay, D. B. (1993) Threonine 204 of the chaperone protein Hsc70 influences the structure of the active site, but is not essential for ATP hydrolysis, *J. Biol. Chem. 268*, 24323−24329.
46. Zhang, Y., and Zuiderweg, E. R. (2004) The 70-kDa heat shock protein chaperone nucleotide-binding domain in solution unveiled as a molecular machine that can reorient its functional subdomains, *Proc. Natl. Acad. Sci. U.S.A. 101*, 10272−10277.
47. Delaglio, F., Grzesiek, S., Vuister, G. W., Zhu, G., Pfeifer, J., and Bax, A. (1995) NMRPipe: a multidimensional spectral processing system based on UNIX pipes, *J. Biomol. NMR 6*, 277−293.
48. Goddard, T. D., and Kneller, D. G. (2000) SPARKY, University of California, San Francisco.
49. Pervushin, K., Riek, R., Wider, G., and Wüthrich, K. (1997) Attenuated T2 relaxation by mutual cancellation of dipole-dipole coupling and chemical shift anisotropy indicates an avenue to NMR structures of very large biological macromolecules in solution, *Proc. Natl. Acad. Sci. U.S.A. 94*, 12366−12371.
50. Lanzetta, P. A., Alvarez, L. J., Reinach, P. S., and Candia, O. A. (1979) An improved assay for nanomole amounts of inorganic phosphate, *Anal. Biochem. 100*, 95−97.
51. Lill, R., Dowhan, W., and Wickner, W. (1990) The ATPase activity of SecA is regulated by acidic phospholipids, SecY, and the leader and mature domains of precursor proteins, *Cell 60*, 271−280.
52. Xiao, B., Spencer, J., Clements, A., Ali-Khan, N., Mittnacht, S., Broceno, C., Burghammer, M., Perrakis, A., Marmorstein, R., and Gamblin, S. J. (2003) Crystal structure of the retinoblastoma tumor suppressor protein bound to E2F and the molecular basis of its regulation, *Proc. Natl. Acad. Sci. U.S.A. 100*, 2363−2368.
53. Lee, G. I., Ding, Z., Walker, J. C., and Van Doren, S. R. (2003) NMR structure of the forkhead-associated domain from the Arabidopsis receptor kinase-associated protein phosphatase, *Proc. Natl. Acad. Sci. U.S.A. 100*, 11261−11266.
54. Landgraf, R., Fischer, D., and Eisenberg, D. (1999) Analysis of heregulin symmetry by weighted evolutionary tracing, *Protein Eng. 12*, 943−951.

55. Berjanskii, M. V., Riley, M. I., and Van Doren, S. R. (2002) Hsc70-interacting HPD loop of the J domain of polyomavirus T antigens fluctuates in psec to nsec and μsec to msec, *J. Mol. Biol. 321*, 503−516.
56. Rubin, S. M., Gall, A. L., Zheng, N., and Pavletich, N. P. (2005) Structure of the Rb C-terminal domain bound to E2F1-DP1: a mechanism for phosphorylation-induced E2F release, *Cell 123*, 1093−1106.
57. Li, X., Romero, P., Rani, M., Dunker, A. K., and Obradovic, Z. (1999) Predicting Protein Disorder for N-, C-, and Internal Regions, *Genome Inf. Ser. 10*, 30−40.
58. Romero, P., Obradovic, Z., Li, X., Garner, E. C., Brown, C. J., and Dunker, A. K. (2001) Sequence complexity of disordered protein, *Proteins 42*, 38−48.
59. Romero, P., Obradovic, Z., and Dunker, A. K. (2004) Natively disordered proteins: functions and predictions, *Appl. Bioinf. 3*, 105−113.
60. Thulasiraman, V., Yang, C. F., and Frydman, J. (1999) In vivo newly translated polypeptides are sequestered in a protected folding environment, *EMBO J. 18*, 85−95.
61. Sadis, S., and Hightower, L. E. (1992) Unfolded proteins stimulate molecular chaperone Hsc70 ATPase by accelerating ADP/ATP exchange, *Biochemistry 31*, 9406−9412.
62. Chesnokova, L. S., and Witt, S. N. (2005) Switches, catapults, and chaperones: steady-state kinetic analysis of Hsp70-substrate interactions, *Biochemistry 44*, 11224−11233.
63. Riley, M. I., Yoo, W., Mda, N. Y., and Folk, W. R. (1997) Tiny T antigen: an autonomous polyomavirus T antigen amino-terminal domain, *J. Virol. 71*, 6068−6074.
64. Qian, Y. Q., Patel, D., Hartl, F.-U., and McColl, D. J. (1996) Nuclear magnetic resonance solution structure of the human Hsp40 (HDJ-1) J-domain, *J. Mol. Biol. 260*, 224−235.
65. Pellecchia, M., Szyperski, T., Wall, D., Georgopoulos, C., and Wüthrich, K. (1996) NMR structure of the J-domain and the Gly/Phe-rich region of the *Escherichia coli* DnaJ chaperone, *J. Mol. Biol. 260*, 236−250.
66. Cook, D. N., and Hassell, J. A. (1990) The amino terminus of polyomavirus middle T antigen is required for transformation, *J. Virol. 64*, 1879−1887.
67. Glenn, G. M., and Eckhart, W. (1995) Amino-terminal regions of polyomavirus middle T antigen are required for interactions with protein phosphatase 2A, *J. Virol. 69*, 3729−3736.
68. Porras, A., Bennett, J., Howe, A., Tokos, K., Bouck, N., Henglein, B., Sathyamangalam, S., Thimmapaya, B., and Rundell, K. (1996) A novel simian virus 40 early-region domain mediates transactivation of the cyclin A promoter by small-t antigen and is required for transformation in small-t antigen-dependent assay, *J. Virol. 70*, 6902−6908.
69. Gruschus, J. M., Greene, L. E., Eisenberg, E., and Ferretti, J. A. (2004) Experimentally biased model structure of the Hsc70/auxilin complex: substrate transfer and interdomain structural change, *Protein Sci. 13*, 2029−2044.
70. Berjanskii, M. V., Riley, M. I., and Van Doren, S. R. (2002) Hsc70-interacting HPD loop of the J domain of polyomavirus T antigens fluctuates in psec to nsec and μsec to msec, *J. Mol. Biol. 321*, 503−516.
71. Sheng, Q., Love, T. M., and Schaffhausen, B. (2000) J domain-independent regulation of the Rb family by polyomavirus large T antigen, *J. Virol. 74*, 5280−5290.
72. Love, T. M., de Jesus, R., Kean, J. A., Sheng, Q., Leger, A., and Schaffhausen, B. (2005) Activation of CREB/ATF sites by polyomavirus large T antigen, *J. Virol. 79*, 4180−4190.
73. Damania, B., and Alwine, J. C. (1996) TAF-like function of SV40 large T antigen, *Genes Dev. 10*, 1369−1381.
74. Damania, B., Mital, R., and Alwine, J. C. (1998) Simian virus 40 large T antigen interacts with human TFIIB-related factor and small nuclear RNA-activating protein complex for transcriptional activation of TATA-containing polymerase III promoters, *Mol. Cell. Biol. 18*, 1331−1338.
75. Alfano, C., and McMacken, R. (1989) Heat shock protein-mediated disassembly of nucleoprotein structures is required for the initiation of bacteriophage lambda DNA replication, *J. Biol. Chem. 264*, 10709−10718.
76. Zylicz, M., Ang, D., Liberek, K., and Georgopoulos, C. (1989) Initiation of lambda DNA replication with purified host- and bacteriophage-encoded proteins: the role of the dnaK, dnaJ and grpE heat shock proteins, *EMBO J. 8*, 1601−1608.
77. Wickner, S., Hoskins, J., and McKenney, K. (1991) Function of DnaJ and DnaK as chaperones in origin-specific DNA binding by RepA, *Nature 350*, 165−167.
78. Wickner, S., Skowyra, D., Hoskins, J., and McKenney, K. (1992) DnaJ, DnaK, and GrpE heat shock proteins are required in oriP1 DNA replication solely at the RepA monomerization step, *Proc. Natl. Acad. Sci. U.S.A. 89*, 10345−10349.
79. Lee, C., Chang, J. H., Lee, H. S., and Cho, Y. (2002) Structural basis for the recognition of the E2F transactivation domain by the retinoblastoma tumor suppressor, *Genes Dev. 16*, 3199−3212.

BI060411D